Inorganic Chemistry

ARTICLE

pubs.acs.org/IC

Seminaphthofluorescein-Based Fluorescent Probes for Imaging Nitric Oxide in Live Cells

Michael D. Pluth, Maria R. Chan, Lindsey E. McQuade, and Stephen J. Lippard*

Department of Chemistry, Massachusetts Institute of Technology, Cambridge, Massachusetts 02139, United States

Supporting Information

ABSTRACT: Fluorescent turn-on probes for nitric oxide based on seminaphthofluorescein scaffolds were prepared and spectroscopically characterized. The Cu(II) complexes of these fluorescent probes react with NO under anaerobic conditions to yield a 20−45-fold increase in integrated emission. The seminaphthofluorescein-based probes emit at longer wavelengths than the parent FL1 and FL2 fluorescein-based generations of NO probes, maintaining emission maxima between 550 and 625 nm. The emission profiles depend on the excitation wavelength; maximum fluorescence turn-on is achieved at excitations between 535 and 575 nm. The probes are highly selective for NO over other biologically relevant reactive nitrogen and oxygen species including NO_3^-, NO_2^-, HNO, $ONOO^-$, NO_2, OCl^-, and H_2O_2. The seminaphthofluorescein-based probes can be used to visualize endogenously produced NO in live cells, as demonstrated using Raw 264.7 macrophages.

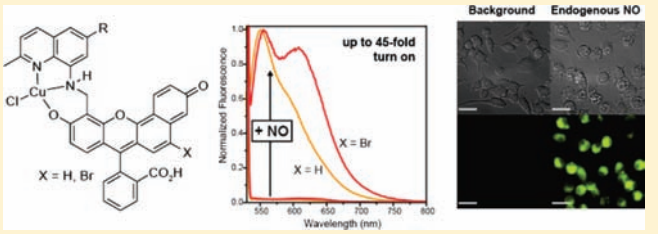

INTRODUCTION

The multifaceted roles of biological nitric oxide (NO) have continued to emerge since the initial discovery that NO is the endothelium-derived relaxing factor (EDRF).[1−3] Subsequent studies revealed that nitric oxide is an important signaling molecule in the immune, cardiovascular, and nervous systems.[4−6] The delicate balance of NO production, action, and translocation requires tight regulation because a breakdown in NO homeostasis is associated with a variety of pathological conditions ranging from carcinogenesis to neurodegradation.[7−13] In order to advance our understanding of pivotal roles played by NO in plants, bacteria, invertebrates, and mammals, chemists have devised strategies to detect this important biological messenger.[6,14−19] Although several strategies are currently employed to detect NO either directly or indirectly, the use of fluorescent probes offers distinct advantages, including high sensitivity and convenience when applied using common microscopic techniques, to yield valuable spatiotemporal information about biologically generated NO.

Fluorescent probes based on small molecule fluorophores, single-walled carbon nanotubes (SWNTs), and proteins have been reported.[20−31] Small molecule fluorescent probes typically rely on one of two strategies for NO detection. The first strategy utilizes organic moieties with electron-rich components, such as 1,2-diaminobenzenes, that react with an oxidation product of NO, such as N_2O_3, to form an electron-deficient product, such as a triazole, to modulate the emission of the fluorophore.[22,32−35] Although such probes comprise the majority of small molecule fluorescent sensors for NO, their inability to react with NO directly, relying on an indirect response that requires a sufficiently oxygenated environment to function, is a liability. The second main strategy used in the preparation of small-molecule-based NO probes is to employ transition metals to modulate the fluorescence of a pendant fluorophore. In contrast to purely organic NO probes, metal-based probes detect NO directly. The close proximity of a transition metal can either quench the fluorescence of a pendant fluorophore until it reacts with NO or facilitate reaction of NO with a dye component. Metal-based fluorescent probes include those based on Co(II), Fe(II), Ru(II), Cu(II), or Rh(II).[32,36−41]

Previously, we reported FL1 and FL2 fluorescent probe families for imaging endogenous nitric oxide in live cells and tissue; these sensors employ Cu(II) to modulate NO reactivity.[25,36,42−45] The probes bind Cu(II) at an 8-aminoquinaldine unit appended to the fluorophore. Upon treatment with NO under anaerobic conditions, the Cu(II) ion is reduced to Cu(I) with concomitant nitrosation of the secondary nitrogen to form the fluorescent nitrosamine product (Figure 1).[43,46] Probes from the CuFL1 and CuFL2 families can detect endogenous NO in cell culture and live tissue slices, emitting in the region of the spectrum typical for fluorescein-based dyes, with maxima near 525 nm. To improve the utility of these NO probes, scaffolds that emit at longer wavelengths are desirable. Such probes would not only expand the palette of colors available for multidye imaging experiments but also require lower energy excitation and thus diminish tissue damage. Furthermore, longer wavelength probes facilitate deeper imaging in live tissue slices or live animals. To address these goals, the FL1 scaffold was modified to emit at longer wavelengths by extending the fluorescein system to a seminaphthofluorescein moiety. Here, we report the synthesis, photophysical characterization, and cellular

Received: May 10, 2011
Published: September 07, 2011

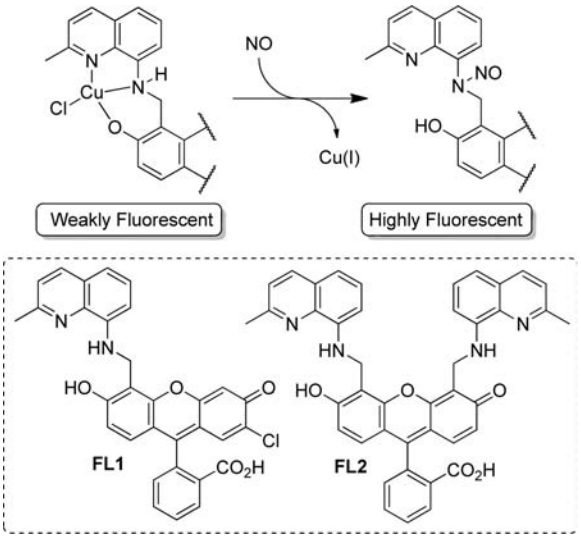

Figure 1. Schematic showing the mechanism of fluorescence response for Cu(II)-based NO probes such as FL1 and FL2.

imaging experiments of a family of seminaphthofluorescein-based SNFL probes that are selective for nitric oxide.

RESULTS AND DISCUSSION

To extend the emission wavelengths of the FL1 family of NO probes, we adopted similar synthetic methodologies to extend the π-system by incorporation of a seminaphthofluorescein moiety. Seminaphthofluorescein dyes have been used as fluorescent probes for numerous biological applications including metal ion detection and pH measurements.[47−53] Such dyes typically emit between 550 and 625 nm, values compatible with common yellow or orange filter sets in fluorescence microscopes.

Synthesis. The first step in the synthesis of the seminaphthofluorescein NO probes involved bromination of the benzoate derivative **1** to form the desired bromomethyl species **3** (Scheme 1).[53] During this reaction, we noticed that an excess of brominating agent **2** and extended times resulted in overbromination to yield **4**. The position of the bromine atom was confirmed by 2D NMR spectroscopy and single crystal X-ray crystallography (Supporting Information Figures S1−S3, Table S1). Kornblum oxidation of the bromomethyl derivative **3** and **4** yielded the respective aldehydes **5** and **6**, which were coupled to substituted 8-aminoquinaldines (**7**, **8**) by reductive amination to yield the final constructs SNFL1, SNFL1E, SNFL1^{Br}, and SNFL1E^{Br}.

Photophysical Properties. The seminaphthofluorescein probes show two overlapping bands in the UV−vis spectrum at ~495/520 nm for SNFL1 (ε_{496} = 8500 ± 100 M^{-1} cm^{-1}, ε_{517} = 8700 ± 100 M^{-1} cm^{-1}) and SNFL1E (ε_{496} = 5030 ± 40 M^{-1} cm^{-1}, ε_{519} = 5200 ± 50 M^{-1} cm^{-1}) and at ~505/530 nm for the brominated analogs SNFL1^{Br} (ε_{505} = 4450 ± 50 M^{-1} cm^{-1}, ε_{530} = 4650 ± 40 M^{-1} cm^{-1}) and SNFL1E^{Br} (ε_{501} = 4070 ± 40 M^{-1} cm^{-1}, ε_{532} = 3930 ± 30 M^{-1} cm^{-1}). The Cu(II) complexes display slight bathochromic shifts in absorbance maxima but otherwise have photophysical properties similar to those of the free ligands (Table 1). Excitation at either of the absorbance maxima results in weak emission in the range 535−545 nm, corresponding to the off-states of the probes.

Upon reaction with nitric oxide, the fluorescence of the Cu(II)-bound seminaphthofluorescein probes increased significantly. For

Scheme 1. Preparation of the Seminaphthofluorescein Family of Probes for Nitric Oxide (see Experimental Section for conditions)

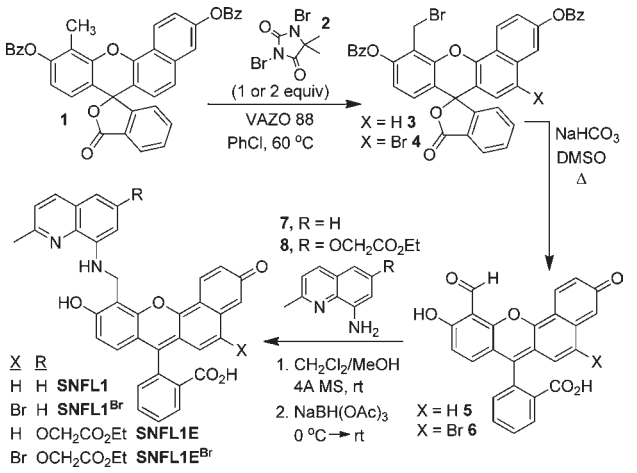

all probes, the emission profile changes dramatically with the excitation wavelength (Figure 2, Supporting Information Figure S4). For example, excitation of SNFL1 and SNFL1E between 500 and 535 nm results in an emission maximum near 545 nm and a strong shoulder at 585 nm. Excitation at longer wavelengths between 535 and 550 nm, however, results in weak emission at 620 nm. The emission properties of SNFL1^{Br} and SNFL1E^{Br} are more complex than those of the nonbrominated analogs. At shorter wavelength excitations, up to 525 nm, the emission maximum is at 550 nm with a weaker band near 600 nm. Above 530 nm excitation, the principal emission band at 550 nm decreases and the main emission shifts to 615 nm (Figure 2). Detailed 2D excitation/emission plots for all of the probes both before and after reaction with NO are supplied in the Supporting Information (Figure S4).

By integrating the emission in both the on and off states of the probes as a function of excitation wavelength, the excitation-dependent magnitude of fluorescence turn-on was determined. For SNFL1, the fluorescence response to NO is maximal in the range between 525 and 535 nm with a net turn-on of 20-fold (42-fold for SNFL1E). SNFL1^{Br} reaches a maximum turn-on of 22-fold (36-fold for SNFL1E^{Br}) after reaction with NO near 535−575 nm. For comparison with the magnitude of turn-on using previously reported NO probes, a similar analysis was performed for FL2. A fluorescence turn-on of 23-fold had been observed using an excitation wavelength of 470 nm. Measurements of the fluorescence turn-on as a function of excitation revealed that, at λ_{ex} = 515 nm, there is a 92-fold increase in integrated emission.

Selectivity for NO over other RONS. Because a variety of reactive oxygen and nitrogen species (RONS) involved in biological processes are associated with nitric oxide, the NO selectivity of the seminaphthofluorescein probes was determined (Figure 3). Because of the excitation wavelength dependence of the turn-on with NO, the response to RONS was monitored at various excitation wavelengths (Figure 3, top). For comparison between the probes, λ_{ex} = 530 nm was used (Figure 3, bottom). Addition of either NO or *S*-nitroso-*N*-acetyl-DL-penicillamine (SNAP), a common NO donor, resulted in a large 20−45-fold increase in integrated emission. This turn-on with 100 equiv of SNAP was identical to that observed after treatment with 1300 equiv of NO.

dx.doi.org/10.1021/ic200986v |*Inorg. Chem.* 2011, 50, 9385–9392

Table 1. Photophysical Properties of Seminaphthofluorescein NO Probes and Representative Properties of FL1 and FL2 Probes for Comparison[a]

	absorption λ_{max} (nm), ε ($\times 10^{-4}$ M^{-1} cm^{-1})		emission λ_{max} (nm), Φ^b(%)		
	unbound	+Cu(II)[c]	unbound	+Cu(II)[c]	+NO[d]
FL1[36]	504, 4.2 ± 0.1	499, 4.0 ± 0.1	520, 7.7 ± 0.2	520, not reported	526, 58 ± 2
FL1E[45]	506, 2.08 ± 0.05	500, 0.77 ± 0.01	520, 2.57 ± 0.02	520, 3.37 ± 0.08	526, 22 ± 1
FL2[25]	498, 2.91 ± 0.07	494, 1.14 ± 0.07	515, 0.74 ± 0.05	512, 0.76 ± 0.04	526, 51 ± 7
FL2E[44]	500, 1.79 ± 0.07	496, 1.12 ± 0.06	522, 0.37 ± 0.05	522, 0.72 ± 0.04	526, 40 ± 8
SFNL1	496, 0.85 ± 0.01	502, 0.468 ± 0.006	542, 2.7 ± 0.4	538, 2.1 ± 0.1	548[h] 22 ± 1
	517, 0.87 ± 0.01	527, 0.507 ± 0.006	544, 2.1 ± 0.1	543, 0.96 ± 0.04	
SNFL1E	496, 0.503 ± 0.004	504, 0.203 ± 0.002	541, 0.9 ± 0.1	538, 0.92 ± 0.09	549[h] 24 ± 2
	519, 0.520 ± 0.005	522, 0.408 ± 0.004	548, 0.72 ± 0.07	543, 0.59 ± 0.04	
$SNFL1^{Br}$	505, 0.445 ± 0.005	504, 0.477 ± 0.007	544, 1.2 ± 0.2	542, 0.34 ± 0.02	548/597[g,i,j] 14 ± 1
	530, 0.465 ± 0.004	540, 0.54 ± 0.01	546, 0.9 ± 0.1	546, 0.14 ± 0.01	
$SNFL1E^{Br}$	501, 0.407 ± 0.004	505, 0.47 ± 0.01	0.49 ± 0.06[e]	0.34 ± 0.01[f]	549/597[g,i,j] 13 ± 1
	532, 0.393 ± 0.003	536, 0.51 ± 0.01	0.25 ± 0.03[e]	0.12 ± 0.01[f]	

[a] Spectroscopic measurements were performed in 50 mM PIPES and 100 mM KCl buffer at pH 7.0 at 25 °C. [b] Quantum yields are based on fluorescein (Φ = 0.95 in 0.1 N NaOH) or rhodamine B (Φ = 0.54 in H_2O). [c] One equivalent of $CuCl_2$ was added per copper-binding site. [d] 1300 equiv of NO, 60 min at 37 °C. Complexes generated in situ. [e] Broad emission, λ_{max} ± 5 nm. [f] The broad emission prevented meaningful λ_{max} determination. [g] $\lambda_{max}(UV) = \lambda_{ex}$ = 517 nm. [h] $\lambda_{max}(UV) = \lambda_{ex}$ = 527 nm. [i] The two emission maxima are of approximately equal intensity. [j] $\lambda_{ex} \geq$ 530 nm results in an emission maxima at 615 nm.

Furthermore, all probes reached a maximum and constant fluorescent state within 1 h of treatment with either SNAP or NO. By contrast, treatment with RONS such as NO_3^-, NO_2^-, $ONOO^-$, HNO, H_2O_2, or OCl^- did not result in fluorescence enhancement. Nitrogen dioxide (NO_2), an oxidation product of NO that can directly nitrosate secondary amines, afforded minimal fluorescence turn-on. These results demonstrate the high selectivity of the seminaphthofluorescein probes for NO over other potential RONS in biological systems.

pH Dependence. Much like the fluorescein-based FL1 and FL2 scaffolds, the emission of the seminaphthofluorescein scaffolds is pH-dependent. To examine the nature of this dependence, pH titrations were performed for SNFL1 and $SNFL1^{Br}$ using both UV−vis and fluorescence spectroscopy. The pH titrations were performed for the metal-free forms of the ligands to remove the Cu-binding equilibrium from the measurement. For both probes, the emission was highest in the 6−8 pH range, a region compatible for most biological experiments (Figure 4, left). For SNFL1, the UV−vis spectrum revealed a pK_a of 7.3 (Figure 4, right). Similarly, measuring the integrated fluorescence as a function of pH revealed pK_a values of 4.9, 6.3, and 7.5 (Supporting Information Figure S9). For the $SNFL1^{Br}$ probe, the UV−vis pH titration yielded a pK_a of 7.5, and values of 5.5, 6.8, and 7.5 were determined by fluorescence spectroscopy (Supporting Information Figure S10). Although the fluorescence of SNFL1 and $SNFL1^{Br}$ changes in the physiological pH range 6−8, the magnitude of the change in emission, ∼2-fold, is an order of magnitude less than the fluorescence response of the probe to NO.

Influence of Zn(II) on Fluorescence. Because of the similarity of the seminaphthofluorescein scaffolds to previous Zn(II) sensors developed in our laboratory[53,54] and because NO mediates Zn(II) release from metallothioneins,[55−57] we investigated the potential of Zn(II) to elicit a fluorescence response from the seminaphthofluorescein-based NO probes. In particular, we titrated CuSNFL1 and $CuSNFL1^{Br}$ with Zn(II) and monitored the integrated emission as a function of added Zn(II) (Figure 5). Addition of 1, 5, 10, 50, 100, 500, or 1000 equiv of Zn(II) to a 10 μM solution of the Cu(II)-bound seminaphthofluorescein probes resulted in only negligible fluorescence. Even at 10 mM Zn(II), only a 5.5- and 2.5-fold turn-on, for CuSNFL1 and $CuSNFL1^{Br}$, respectively, was observed. These results reveal that the seminaphthofluorescein probes are more sensitive to NO than to biological concentrations of Zn(II).

Fluorescence Imaging of Endogenous NO. Having demonstrated the efficacy of the seminaphthofluorescein-based probes for NO detection in the cuvette, we next evaluated their biological compatibility by imaging NO produced in live cells. For these studies we investigated Raw 264.7 murine macrophage cells, which generate NO from iNOS upon stimulation with endotoxins and cytokines.[58] Upon addition of lipopolysaccharide (LPS) and interferon-γ (INF-γ), Raw 264.7 cells produce micromolar concentrations of NO and are therefore ideal for evaluating the potential of the seminaphthofluorescein-based probes under biological conditions. Treatment of the cells with only the Cu(II)-bound fluorescent probes resulted in minimal observed emission. By contrast, stimulation with LPS and INF-γ in the presence of the seminaphthofluorescein probes resulted in a significant increase in fluorescence intensity. In all cases, a substantial emission enhancement occurred, thus demonstrating the suitability of the probes for detection of endogenous levels of NO. Representative images of the fluorescence both with and without stimulation of iNOS are presented in Figure 6. Sample line scans showing the magnitude of signal in both sets of cells are also included. Despite the ester functionality on the SNFL1E and $SNFL1E^{Br}$ probes, which is often used to impart cell trappability effected by hydrolysis by intracellular esterases to yield negatively charged carboxylates, the esterified seminaphthofluorescein probes diffused out of the cells in a manner similar to that of the parent SNFL1 and $SNFL1^{Br}$ probes (see Supporting Information Figures S11−S14).

Summary. The synthesis and photophysical properties of seminaphthofluorescein-based fluorescent probes for nitric oxide are reported. Upon reaction with NO, the Cu(II) ligated SNFL1, SNFL1E, $SNFL1^{Br}$, and $SNFL1E^{Br}$ probes exhibit 20−45-fold

dx.doi.org/10.1021/ic200986v |*Inorg. Chem.* 2011, 50, 9385–9392

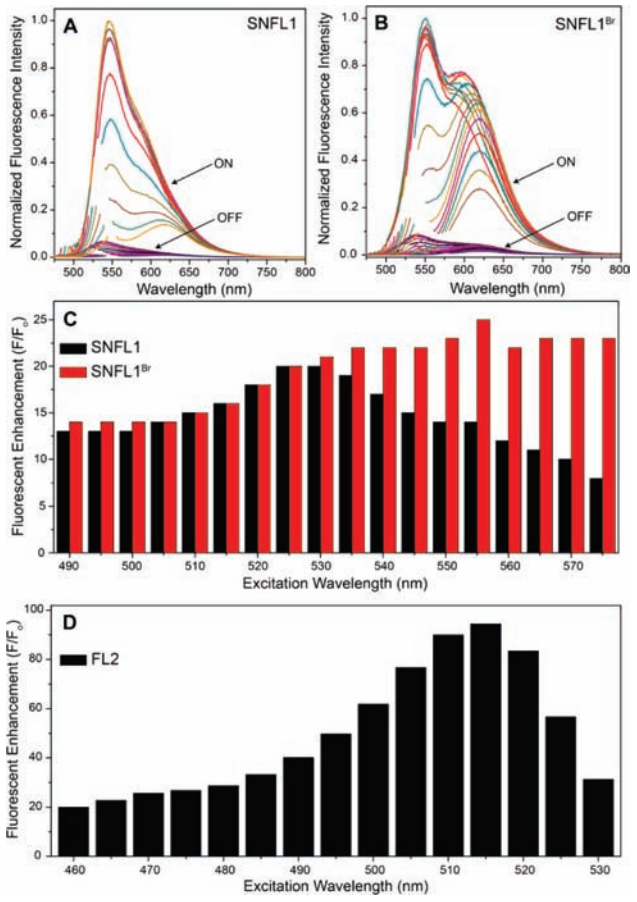

Figure 2. Emission of (a) CuSNFL1 and (b) CuSNFL1^{Br} before and after addition of NO as a function of excitation wavelength. The excitation peaks have been removed for clarity. (c) Integrated fluorescence turn-on as a function of excitation wavelength for CuSNFL1 and CuSNFL1^{Br}. (d) Integrated emission of Cu_2FL2 as a function of wavelength is shown for comparison. Conditions: 1 μM probe, 50 mM PIPES, 100 mM KCl, pH 7, 37 °C, 1300 equiv of NO incubated for 1 h.

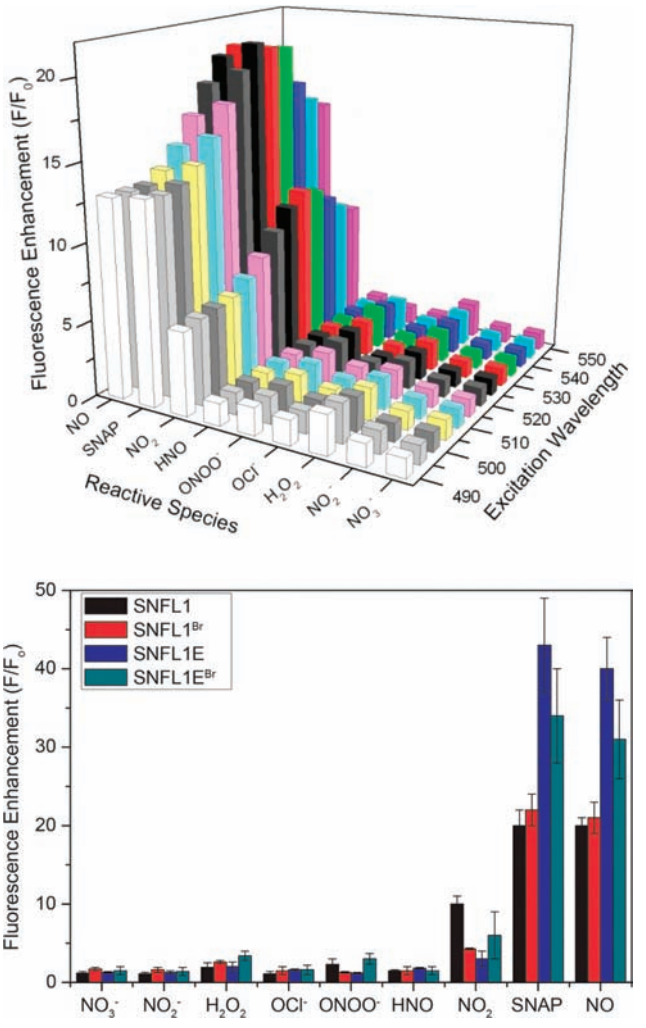

Figure 3. (Top) Selectivity of CuSNFL1 fluorescence response for NO over other reactive nitrogen and oxygen species as a function of excitation wavelength. (Bottom) Comparison of the selectivity for NO over other RONS for CuSNFL1, CuSNFL1^{Br}, CuSNFL1E, and CuSNFL1E^{Br}. Conditions: 50 mM PIPES, 100 mM KCl, pH 7.0, 37 °C, 60 min, 100 equiv of RONS or SNAP, 1300 equiv of NO, λ_{ex} = 530 nm. The selectivity of the probes over a broad range of excitation wavelengths is reported in the Supporting Information (Figures S5−S8 and Tables S2−S5).

increases in integrated fluorescence. All of the probes are highly selective for NO or NO donors over other reactive oxygen and nitrogen species. Treatment of the Cu(II)-bound ligands with a large excess of Zn(II) did not elicit a significant fluorescence response. All of the seminaphthofluorescein probes are cell permeable and can be used to image endogenous levels of NO, as demonstrated in Raw 264.7 murine macrophage cells.

EXPERIMENTAL SECTION

Synthetic Materials and Methods. Seminaphthofluorescein precursors **1**, **3**, and **5**,[53] aminoquinaldines **7**[59] and **8**,[60] and FL2[25] and FL2E[44] were prepared as described previously. Silica gel (SiliaFlash F60, Silicycle, 230−400 mesh) was used for column chromatography. Thin-layer chromatography (TLC) was performed on J. T. Baker 1B−F silica gel plates (250 μm thickness) and viewed by UV illumination. Preparative TLC was performed on Silicycle SiliaPlates (1000 μm thickness). NMR spectra were acquired on a Bruker 400 MHz spectrometer at ambient temperature. Chemical shifts are reported in parts per million (δ) and are referenced to residual protic solvent resonances. The following abbreviations are used in describing NMR couplings: (s) singlet, (d) doublet, (t) triplet, (q) quartet, (b) broad, (m) multiplet. Melting points were measured on a MelTemp apparatus and are reported as

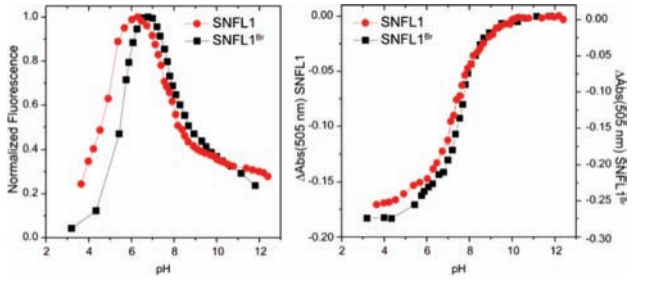

Figure 4. (Left) Integrated fluorescence as a function of pH for SNFL1 and SNFL1^{Br}. (Right) Change in absorbance in the UV−vis spectrum at 505 nm for SNFL1 and SNFL1^{Br} as a function of pH. Conditions: 20 μM dye, 100 mM KCl, 25 °C.

uncorrected temperatures. High-resolution mass spectra were measured by the staff at the MIT Department of Chemistry Instrumentation

dx.doi.org/10.1021/ic200986v |Inorg. Chem. 2011, 50, 9385–9392

Facility (DCIF). Elemental analyses were performed by a commercial analytical laboratory.

Spectroscopic Materials and Methods. Piperazine-*N*,*N*′-bis(2-ethanesulfonic acid) (PIPES, Calbiochem) and potassium chloride (99.999%, Aldrich) were used to make buffered solutions (50 mM PIPES, 100 mM KCl, pH 7.0) with Millipore water. Nitric oxide was purchased from Airgas and was purified as described previously.[61] Nitrogen dioxide (NO_2) was purchased from Aldrich and purified by condensation into a gas bulb at −78 °C followed by exposure to vacuum to remove higher boiling impurities. SNAP, sodium peroxynitrite, sodium nitrite, and Angeli's salt ($Na_2N_2O_3$) were purchased from Cayman Chemical and stored at −80 °C prior to use. Nitric oxide and NO_2, as well as 1.0 mM solutions of other reactive oxygen and nitrogen species (RONS), were introduced into buffered solutions via gastight syringes. Copper(II) chloride dihydrate (99+%, Alfa Aesar) was used to prepare 1.0 mM $CuCl_2$ stock solutions with Millipore water. Stock solutions of the fluorescent probes were prepared in DMSO and stored in aliquots at −80 °C until immediately prior to use. UV−visible spectra were acquired on a Cary 50-Bio or a Cary 1E spectrometer. Acquisitions were made at 25.00 ± 0.05 °C. Fluorescence spectra were obtained on a Quanta Master 4 L-format scanning spectrofluorimeter (Photon Technology International) at 25.0 ± 0.1 or 37.0 ± 0.1 °C. All fluorescence measurements were made under anaerobic conditions, with cuvette solutions prepared in an inert atmosphere glovebox. All UV−vis and fluorescence experiments were repeated at least in triplicate.

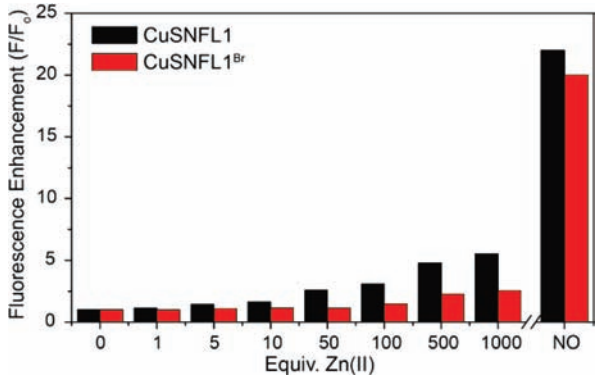

Figure 5. Fluorescence response of CuSNFL1 and CuSNFL1^{Br} to Zn(II). The fluorescence response for NO is shown for comparison. Conditions: 10 μM $CuCl_2$, 10 μM probe, 50 mM PIPES, 100 mM KCl, pH 7.0, 25 °C. The Zn(II) concentration was adjusted with 10 mM or 1.0 mM $ZnCl_2$.

Cell Culture and Imaging Materials and Methods. Raw 264.7 murine macrophages were obtained from ATCC and were cultured in Dulbecco's modified Eagle medium (DMEM, Cellgro, MediaTek, -Inc.) supplemented with 10% fetal bovine serum (FBS, HyClone), 1% penicillin−streptomycin, 1% sodium pyruvate (Cellgro, MediaTek, Inc.), and 1% MEM nonessential amino acids (Sigma). For imaging studies, cells grown to confluence were passed and plated into poly-D-lysine coated plates (MatTek) containing 2 mL of DMEM. After incubation at 37 °C with 5% CO_2 for at least 5 h, the media was removed, the cells were washed with 2 mL of PBS buffer, and 2 mL of fresh DMEM was added along with the fluorescent probes and/or iNOS stimulants. Cells were incubated for 14−16 h prior to imaging. For all cell studies, the Cu(II) complexes of the fluorescent probes were generated in situ by combining stock solutions of $CuCl_2$ and the dye. For all comparison studies, the plates were loaded with identical volumes from the same cell stock solution to ensure that an equal number of cells were passed to each plate.

For nitric oxide detection studies, NO production by iNOS was induced in Raw 264.7 macrophages with 0.75 ng/mL of lipopolysaccharide (LPS, Sigma) and 495−4950 U/mL of interferon-gamma (IFN-γ, BD Biosciences). The concentrations of LPS and INF-γ were optimized using Cu_2FL2E. Cells were then coincubated with either 2 μM CuSNFL1, 2 μM CuSNFL1^{Br}, 4 μM CuSNFL1E, or 4 μM CuSNFL1E^{Br} and 4.5 μM Hoechst 33258 (Sigma). Prior to imaging, cells were washed with 2 mL of PBS and then bathed in 2 mL of warm PBS during imaging.

Fluorescence Microscopy. Images were acquired on a Zeiss Axiovert 200 M inverted epifluorescence microscope equipped with an EM-CCD digital camera (Hamamatsu) and an X-Cite 120 metal halide lamp (EXFO). Differential interference contrast (DIC) and fluorescence images were obtained using an oil immersion 63× objective lens, with exposure time ranging from 250 ms to 1.75 s. Emission from the seminaphthofluorescein-based probes was detected using a custom filter set (Chroma) with a 500 nm excitation filter (HQ500/40×), a 530 nm dichroic mirror (Q530LP), and a 550 nm long pass emission filter (E550LP). The microscope was operated with Volocity software

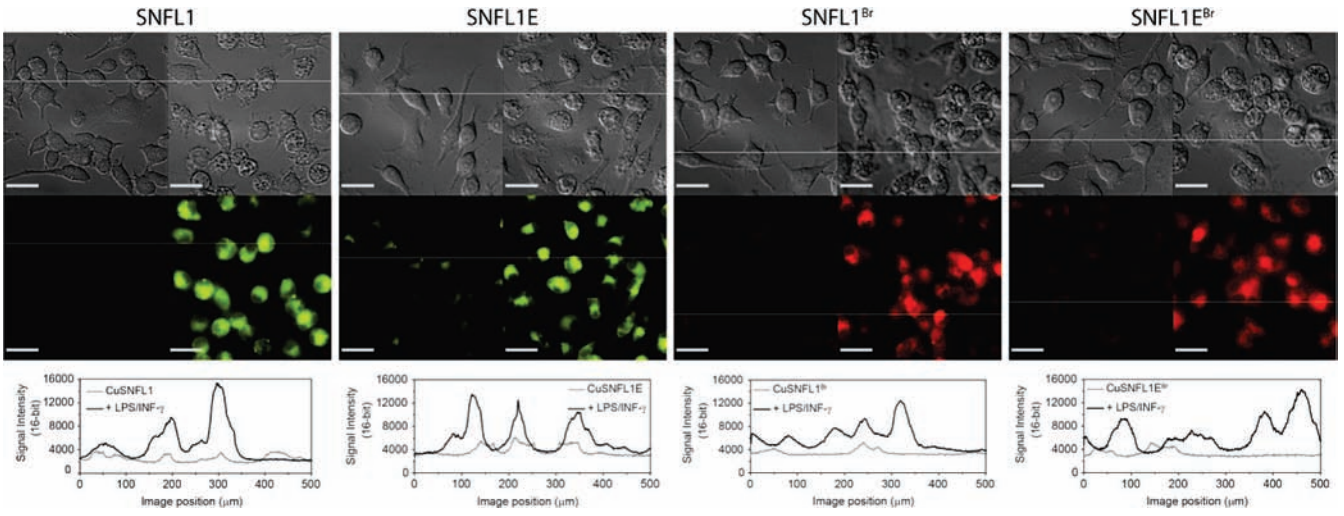

Figure 6. Fluorescence imaging of endogenous NO produced in Raw 264.7 cells. For each set of images, the left image corresponds to treatment with the fluorescent probe only. Images in the right panel correspond to cells treated with the fluorescent probes and stimulated with LPS and INF-γ. (Top) DIC images. (Bottom) Fluorescence images. The fluorescence intensity of the uncorrected fluorescence images are shown below to compare the fluorescence response in unstimulated and stimulated cells. [Probe] = 2 μM for CuSNFL1 and CuSFNL1^{Br}, 4 μM for CuSNFL1E and CuSNFL1E^{Br}. [LPS] = 0.75 ng/mL, [INF-γ] = 495−4950 U/mL, incubation for 14−16 h. Scale bars = 23 μm.

dx.doi.org/10.1021/ic200986v |*Inorg. Chem.* 2011, 50, 9385–9392

(Improvision) and images were analyzed with either the Volocity software or ImageJ.[62] All fluorescent images were corrected for background. Uncorrected images are shown in the Supporting Information (Figures S15−S18).

X-ray Data Collection and Structure Solution Refinement. Crystals of **6** of suitable quality for X-ray diffraction were grown by diffusion of hexanes into a $CHCl_3$ solution of **6**. A single crystal was mounted in Paratone N oil using a 30 μm aperture MiTeGen MicroMounts (Ithaca, NY) loop and frozen under a nitrogen cold stream maintained by a KRYO-FLEX low-temperature apparatus set to 100 K. Data were collected on a Bruker SMART APEX CCD X-ray diffractometer with Mo Kα radiation (λ = 0.710 73 Å) controlled by the APEX2 software package (v 2010).[63] Data reduction was performed with SAINT and empirical absorption corrections were applied with SADABS.[64] The structures were solved by direct methods with refinement by full-matrix least-squares based on F^2 using SHELXTL-97.[65,66] All non-hydrogen atoms were located and their positions refined anisotropically. Hydrogen atoms were assigned to idealized positions and given thermal parameters equal to 1.2 times the thermal parameters of the atoms to which they were attached.

Syntheses. *8-Bromo-11-(bromomethyl)-3′-oxo-3′H-spiro[benzo[c]xanthene-7,1′-isobenzofuran]-3,10-diyl Dibenzoate,* ***4***. A mixture of dibenzoate **1** (11.9 g, 19.7 mmol), 1,3-dibromo-5,5-dimethyl hydantoin **2** (12.7 g, 44.4 mmol), VAZO 88 (660 mg, 2.71 mmol), and glacial acetic acid (420 μL, 7.3 mmol) was added to 300 mL of chlorobenzene and heated at 60 °C for 7 days. The resultant solution was washed with hot water and dried with $MgSO_4$, and the solvents were removed under vacuum. The resultant solid was recrystallized from a minimal amount of toluene and ethanol (~10:1) to yield the desired product (13.4 g, 89% yield). Note: If the bromination does not go to completion, excess VAZO 88 or **2** can be added during the course of the reaction. Mp: 171−173 °C (dec). ^{1}H NMR (400 MHz, $CDCl_3$): δ 8.72 (d, J = 8.8, 1H, Ar*H*), 8.24 (d, J = 7.2, 4H, Ar*H*), 8.06 (m, 2H, Ar*H*), 7.67 (m, 5H, Ar*H*), 7.52 (m, 4H, Ar*H*), 7.20 (d, J = 8.0, 1H, Ar*H*), 7.11 (s, 1H, Ar*H*), 7.06 (d, J = 8.8, 1H, Ar*H*), 6.91 (d, J = 8.4, 1H, Ar*H*) 4.88 (m, 2H, CH_2). ^{13}C{^{1}H} NMR (100 MHz, $CDCl_3$): δ 169.2, 165.2, 164.4, 152.9, 152.0, 149.4, 146.3, 135.5, 134.5, 134.2, 130.7, 130.6, 130.5, 129.24, 129.17, 129.10, 128.92, 128.7, 128.1, 126.1, 125.7, 124.7, 124.4, 123.7, 123.1, 119.35, 119.30, 119.22, 117.16, 117.05, 113.51, 81.7, 20.5. HRMS ([M + H]$^+$): calcd m/z 760.9805, found m/z 760.9827. Anal. Calcd for $C_{39}H_{22}Br_2O_7$EtOH: C, 60.91; H, 3.49. Found: C, 60.81; H, 3.21.

2-(11-Formyl-10-hydroxy-8-bromo-3-oxo-3H-benzo[c]xanthen-7-yl)benzoic Acid, ***6***. The seminaphthofluorescein bromide **4** (2.0 g, 2.9 mmol) was combined with $NaHCO_3$ (2.0 g, 24 mmol) in 70 mL of DMSO and heated to 140 °C for 3 h. The reaction mixture was cooled to room temperature, poured into 350 mL of 4 M HCl, and stirred for 30 min. The solution was filtered, washed with water, and dried under vacuum. The resultant crude product was purified using two SiO_2 columns. The first column was eluted with 10% MeOH in CH_2Cl_2. The second column was eluted with 2% MeOH in CH_2Cl_2 to yield the pure aldehyde **6** (59 mg, 5% yield). Mp: >300 °C. ^{1}H NMR (400 MHz, 10:1 CD_2Cl_2:MeOD-d_4): δ 8.35 (d, J = 9.2, 1H, Ar*H*), 8.06 (d, J = 7.6, 1H, Ar*H*), 7.72 (m, 2H, Ar*H*), 7.45 (s, 1H, Ar*H*), 7.29 (d, J = 9.2, 1H, Ar*H*), 7.17 (d, J = 7.6, 1H, Ar*H*), 6.96 (s, 1H, Ar*H*), 6.93 (d, J = 9.2, 1H, Ar*H*), 6.66 (d, J = 9.2, 1H, Ar*H*). ^{13}C{^{1}H} NMR (100 MHz, 10:1 CD_2Cl_2:d_4-MeOD): δ 193.5, 170.2, 164.8, 159.3, 153.1, 153.0, 146.5, 137.5, 136.5, 135.5, 131.1, 127.8, 126.9, 125.9, 124.8, 124.6, 120.4, 119.3, 116.8, 114.8, 111.3, 111.3, 111.1, 109.8, 82.8. HRMS ([M + H]$^+$): calcd m/z 488.9968, found m/z 488.9954. Anal. Calcd for $C_{25}H_{13}BrO_6$·MeOH: C, 59.90; H, 3.29; Found: C, 60.13; H, 3.66.

2-(10-Hydroxy-11-(((2-methylquinolin-8-yl)amino)methyl)-3-oxo-3H-benzo[c]xanthen-7-yl)benzoic Acid, SNFL1. The seminaphthofluorescein aldehyde **5** (13.4 mg, 32.7 μmol) and 2-methylquinolin-8-amine **7** (6.2 mg, 49 μmol) were combined in 2 mL of anhydrous MeOH and 2 mL of anhydrous CH_2Cl_2 containing 4 Å molecular sieves. The solution was protected from light and stirred for 1 h, after which the reaction solution was cooled to 0 °C. Next, $NaBH(OAc)_3$ (34 mg, 163 μmol) was added in one portion. The solution was allowed to warm to room temperature and stirred overnight. After filtration and removal of the solvents under vacuum, the residual red solid was dissolved in a minimal amount of MeOH and purified by preparative TLC eluting with 5% MeOH in CH_2Cl_2 to afford SNFL1 (5.9 mg, 30% yield). Mp: 185−187 (dec). ^{1}H NMR (400 MHz, 10:1 CD_2Cl_2:MeOH-d_4): δ 8.38 (d, J = 9.2, 1H, Ar*H*), 8.02 (d, J = 6.8 Hz, 1H, Ar*H*), 7.96 (d, J = 8.4, 1H, Ar*H*), 7.62 (m, 2H, Ar*H*), 7.28 (overlapping m, 3H, Ar*H*), 7.13 (overlapping m, 5H, Ar*H*), 6.69 (d, J = 8.4, 2H, Ar*H*), 6.62 (d, J = 7.2, 1H, Ar*H*), 5.02 (s, 2H, CH_2), 2.54 (s, 3H, CH_3). HRMS ([M − H]$^-$) calcd m/z 551.1612, found m/z 551.1608.

2-(11-(((6-(2-Ethoxy-2-oxoethoxy)-2-methylquinolin-8-yl)amino)-methyl)-10-hydroxy-3-oxo-3H-benzo[c]xanthen-7-yl)benzoic Acid, SNFL1E. The seminaphthofluorescein aldehyde **5** (27.0 mg, 65.7 μmol) and aminoquinaldine ester **8** (22.2 mg, 85.7 μmol) were combined in 2 mL of anhydrous MeOH and 2 mL of anhydrous CH_2Cl_2 containing 4 Å molecular sieves. The solution was protected from light and stirred for 2 h, after which the reaction solution was cooled to 0 °C. After cooling, $NaBH(OAc)_3$ (25.1 mg, 118 μmol) was added in one portion. The solution was allowed to warm to room temperature and stirred for 3 h. After filtration and removal of the solvents under vacuum, the red residual solid was dissolved in a minimal amount of MeOH and purified by preparative TLC eluting with 8% MeOH in CH_2Cl_2 to yield SNFL1E (8.9 mg, 16% yield). Mp: 174−177 °C (dec). ^{1}H NMR (400 MHz, 10:1 CD_2Cl_2:MeOH-d_4): δ 8.45 (d, J = 8.8 Hz, 1H, Ar*H*), 8.03 (bs, 1H, Ar*H*), 7.81 (d, J = 8.0 Hz, 1H, Ar*H*), 7.61 (bs, 2H, Ar*H*), 7.27 (d, J = 8.8 Hz, 1H, Ar*H*), 7.17 (m, 3H, Ar*H*), 7.13 (s, 1H, Ar*H*), 6.80 (overlapping m, 3H, Ar*H*), 6.28 (d, J = 8.8 Hz, 1H, Ar*H*), 6.29 (s, 1H, Ar*H*), 4.90 (s, 2H, CH_2), 4.66 (s, 2H, CH_2), 4.22 (q, J = 7.2 Hz, 2H, CH_2), 2.44 (s, 3H, CH_3), 1.26 (t, J = 4.8 Hz, 3H, CH_3). HRMS ([M − H]$^-$): calcd m/z 653.1929, found m/z 653.1936.

2-(8-Bromo-10-hydroxy-11-(((2-methylquinolin-8-yl)amino)methyl)-3-oxo-3H-benzo[c]xanthen-7-yl)benzoic acid, SNFL1^{Br}. The brominated seminaphthofluorescein aldehyde **6** (16.1 mg, 39.2 μmol) and 2-methylquinolin-8-amine **7** (6.8 mg, 43 μmol) were combined in 2 mL of anhydrous MeOH and 3 mL of anhydrous CH_2Cl_2 containing 4 Å molecular sieves. The solution was protected from light and stirred for 3 h, after which the reaction solution was cooled to 0 °C. After cooling, $NaBH(OAc)_3$ (16 mg, 78 μmol) was added in one portion. The solution was allowed to warm to room temperature and stirred overnight. After filtration and removal of the solvents under vacuum, the red residual solid was dissolved in a minimal amount of MeOH and purified by preparative TLC eluting with 10% MeOH in CH_2Cl_2 to yield SNFL1^{Br} (9.3 mg, 41% yield). Mp: 179−181 °C (dec). ^{1}H NMR (400 MHz, 10:1 CD_2Cl_2:MeOH-d_4): δ 8.43 (d, J = 8.4, 1H, Ar*H*), 8.06 (bs, 1H, Ar*H*), 7.95 (d, J = 8.4, 1H, Ar*H*), 7.66 (bs, 2H, Ar*H*), 7.45 (s, 1H, Ar*H*), 7.32 (t, J = 6.4, 1H, Ar*H*), 7.18 (overlapping m, 4H, Ar*H*), 7.09 (d, J = 8.4, 1H, Ar*H*), 7.06 (s, 1H, Ar*H*), 6.73 (d, J = 8.4, 1H, Ar*H*), 6.64 (d, J = 8.4, 1H, Ar*H*), 4.96 (s, 2H, CH_2), 2.50 (s, 3H, CH_3). HRMS ([M + H]$^+$): calcd m/z 631.0863, found m/z 631.0841.

2-(8-Bromo-11-(((6-(2-ethoxy-2-oxoethoxy)-2-methylquinolin-8-yl)-amino)methyl)-10-hydroxy-3-oxo-3H-benzo[c]xanthen-7-yl)benzoic Acid, SFNL1E^{Br}. The brominated seminaphthofluorescein aldehyde **6** (13.1 mg, 31.8 μmol) and aminoquinaldine ester **8** (10.4 mg, 39.4 μmol) were combined in 1 mL of anhydrous MeOH and 1 mL of anhydrous CH_2Cl_2 containing 4 Å molecular sieves. The solution was protected from light and stirred for 2 h, after which the reaction solution was cooled to 0 °C. After cooling, $NaBH(OAc)_3$ (13.5 mg, 63.6 μmol) was added in one portion. The reaction mixture was allowed to warm to room temperature and stirred for 2 h, after which it was filtered, and the solvents were removed under vacuum.

The red residual solid was dissolved in a minimal amount of MeOH and purified by preparative TLC eluting with 6% MeOH in CH_2Cl_2 to yield SNFL1E^{Br} (12 mg, 58% yield). Mp: 169−171 °C (dec). ^{1}H NMR (400 MHz, MeOH-d_4): δ 8.46 (d, J = 8.8, 1H, ArH), 8.05 (dd, J = 6.4, 2.4, 1H, ArH), 7.80 (d, J = 8.4, 1H, ArH), 7.70 (m, 2H, ArH), 7.44 (d, J = 2.0, 1H, ArH), 7.19 (overlapping m, 2H, ArH), 7.12 (d, J = 8.4, 1H, ArH), 6.49 (s, 1H, ArH), 6.87 (d, J = 1.6, 1H, ArH), 6.69 (s, 2H, ArH), 6.35 (d, J = 2.4, 1H, ArH), 4.68 (s, 2H, CH_2), 4.62 (bs, 2H, CH_2), 4.22 (q, J = 6.8 Hz, 2H, CH_2), 2.36 (s, 3H, CH_3), 1.25 (t, J = 6.8, 3H, CH_3). HRMS ([M + H]$^+$): calcd m/z 733.1180, found m/z 733.1177.

■ ASSOCIATED CONTENT

Supporting Information. X-ray crystallographic data of compound **6** in CIF format, excitation/emission plots for all probes, selectivity plots and data for various excitation wavelengths, pH profiles, raw cell images, cell washing studies, NMR spectra. This material is available free of charge via the Internet at http://pubs.acs.org.

■ AUTHOR INFORMATION

Corresponding Author
*E-mail: lippard@mit.edu.

■ ACKNOWLEDGMENT

This work was supported the National Science Foundation (CHE-0611944 to SJL) and the National Institutes of Health (K99GM092970 to MDP). Instrumentation in the MIT DCIF is maintained with funding from NIH grant 1S10RR13886-01. The authors thank Daniela Buccella for helpful discussions and suggestions.

■ REFERENCES

(1) Rapoport, R. M.; Draznin, M. B.; Murad, F. *Nature* **1983**, *306*, 174–176.
(2) Ignarro, L. J.; Buga, G. M.; Wood, K. S.; Byrns, R. E.; Chaudhuri, G. *Proc. Natl. Acad. Sci. U. S. A.* **1987**, *84*, 9265–9269.
(3) Furchgott, R. F.; Vanhoutte, P. M. *FASEB J.* **1989**, 3, 2007–2018.
(4) Ignarro, L. J. *Nitric Oxide Biology and Pathobiology*, 1st ed.; Academic Press: San Diego, 2000.
(5) Garthwaite, J. *E. J. Neurosci.* **2008**, *27*, 2783–2802.
(6) Pluth, M. D.; Tomat, E.; Lippard, S. J. *Annu. Rev. Biochem.* **2011**, *80*, 333–355.
(7) Brown, G. C.; Bal-Price, A. *Mol. Neurobiol.* **2003**, *27*, 325–355.
(8) Heales, S. J. R.; Bolaños, J. P.; Stewart, V. C.; Brookes, P. S.; Land, J. M.; Clark, J. B. *Biochim. Biophys. Acta, Bioenerg.* **1999**, *1410*, 215–228.
(9) Johnson, R. A.; Freeman, R. H. *Am. J. Hypertens.* **1992**, *5*, 919–922.
(10) Oyadomari, S.; Takeda, K.; Takiguchi, M.; Gotoh, T.; Matsumoto, M.; Wada, I.; Akira, S.; Araki, E.; Mori, M. *Proc. Natl. Acad. Sci. U. S. A.* **2001**, *98*, 10845–10850.
(11) Pieper, G. M. *Hypertension* **1998**, *31*, 1047–1060.
(12) Smith, K. J.; Lassmann, H. *Lancet Neurol.* **2002**, *1*, 232–241.
(13) Titheradge, M. A. *Biochim. Biophys. Acta, Bioenerg.* **1999**, *1411*, 437–455.
(14) Ye, X.; Rubakhin, S. S.; Sweedler, J. V. *Analyst* **2008**, *133*, 423–433.
(15) Ghafourifar, P.; Parihar, M. S.; Nazarewicz, R.; Zenebe, W. J.; Parihar, A. In *Nitric Oxide, Part F: Oxidative and Nitrosative Stress in Redox Regulation of Cell Signaling*; Academic Press: New York, 2008; Vol. 440, pp 317−334.
(16) Hetrick, E. M.; Schoenfisch, M. H. *Annu. Rev. Anal. Chem.* **2009**, *2*, 409–433.
(17) McQuade, L. E.; Lippard, S. J. *Curr. Opin. Chem. Biol.* **2010**, *14*, 43–49.
(18) Nagano, T. *J. Clin. Biochem. Nutr.* **2009**, *45*, 111–124.
(19) Nagano, T.; Yoshimura, T. *Chem. Rev.* **2002**, *102*, 1235–1269.
(20) Sasaki, E.; Kojima, H.; Nishimatsu, H.; Urano, Y.; Kikuchi, K.; Hirata, Y.; Nagano, T. *J. Am. Chem. Soc.* **2005**, *127*, 3684–3685.
(21) Kojima, H.; Nakatsubo, N.; Kikuchi, K.; Urano, Y.; Higuchi, T.; Tanaka, J.; Kudo, Y.; Nagano, T. *Neuroreport* **1998**, *9*, 3345–3348.
(22) Kojima, H.; Nakatsubo, N.; Kikuchi, K.; Kawahara, S.; Kirino, Y.; Nagoshi, H.; Hirata, Y.; Nagano, T. *Anal. Chem.* **1998**, *70*, 2446–2453.
(23) Kojima, H.; Sakurai, K.; Kikuchi, K.; Kawahara, S.; Kirino, Y.; Nagoshi, H.; Hirata, Y.; Akaike, T.; Maeda, H.; Nagano, T. *Biol. Pharm. Bull.* **1997**, *20*, 1229–1232.
(24) Sato, M.; Nakajima, T.; Goto, M.; Umezawa, Y. *Anal. Chem.* **2006**, *78*, 8175–8182.
(25) McQuade, L. E.; Lippard, S. J. *Inorg. Chem.* **2010**, *49*, 7464–7471.
(26) Yang, Y. J.; Seidlits, S. K.; Adams, M. M.; Lynch, V. M.; Schmidt, C. E.; Anslyn, E. V.; Shear, J. B. *J. Am. Chem. Soc.* **2010**, *132*, 13114–13116.
(27) Zhang, J. Q.; Boghossian, A. A.; Barone, P. W.; Rwei, A.; Kim, J. H.; Lin, D. H.; Heller, D. A.; Hilmer, A. J.; Nair, N.; Reuel, N. F.; Strano, M. S. *J. Am. Chem. Soc.* **2011**, *133*, 567–581.
(28) Kim, J. H.; Heller, D. A.; Jin, H.; Barone, P. W.; Song, C.; Zhang, J.; Trudel, L. J.; Wogan, G. N.; Tannenbaum, S. R.; Strano, M. S. *Nat. Chem.* **2009**, *1*, 473–481.
(29) Barker, S. L. R.; Clark, H. A.; Swallen, S. F.; Kopelman, R.; Tsang, A. W.; Swanson, J. A. *Anal. Chem.* **1999**, *71*, 1767–1772.
(30) Barker, S. L. R.; Zhao, Y. D.; Marletta, M. A.; Kopelman, R. *Anal. Chem.* **1999**, *71*, 2071–2075.
(31) Sato, M.; Hida, N.; Umezawa, Y. *Proc. Natl. Acad. Sci. U. S. A.* **2005**, *102*, 14515–14520.
(32) Katayama, Y.; Takahashi, S.; Maeda, M. *Anal. Chim. Acta* **1998**, *365*, 159–167.
(33) Kojima, H.; Hirotani, M.; Nakatsubo, N.; Kikuchi, K.; Urano, Y.; Higuchi, T.; Hirata, Y.; Nagano, T. *Anal. Chem.* **2001**, *73*, 1967–1973.
(34) Marzinzig, M.; Nussler, A. K.; Stadler, J.; Marzinzig, E.; Barthlen, W.; Nussler, N. C.; Beger, H. G.; Morris, S. M.; Bruckner, U. B. *Nitric Oxide Biol. Chem.* **1997**, *1*, 177–189.
(35) Nagano, T.; Takizawa, H.; Hirobe, M. *Tetrahedron Lett.* **1995**, *36*, 8239–8242.
(36) Lim, M. H.; Xu, D.; Lippard, S. J. *Nat. Chem. Biol.* **2006**, *2*, 375–380.
(37) Ouyang, J.; Hong, H.; Shen, C.; Zhao, Y.; Ouyang, C. G.; Dong, L.; Zhu, J. H.; Guo, Z. J.; Zeng, K.; Chen, J. N.; Zhang, C. Y.; Zhang, J. F. *Free Radical Biol. Med.* **2008**, *45*, 1426–1436.
(38) Hilderbrand, S. A.; Lim, M. H.; Lippard, S. J. *J. Am. Chem. Soc.* **2004**, *126*, 4972–4978.
(39) Lim, M. H.; Lippard, S. J. *Inorg. Chem.* **2004**, *43*, 6366–6370.
(40) Ortiz, M.; Torrens, M.; Mola, J. L.; Ortiz, P. J.; Fragoso, A.; Diaz, A.; Cao, R.; Prados, P.; de Mendoza, J.; Otero, A.; Antinolo, A.; Lara, A. *Dalton Trans.* **2008**, 3559–3566.
(41) Soh, N.; Katayama, Y.; Maeda, M. *Analyst* **2001**, *126*, 564–566.
(42) Lim, M. H.; Lippard, S. J. *Acc. Chem. Res.* **2007**, *40*, 41–51.
(43) Lim, M. H.; Wong, B. A.; Pitcock, W. H.; Mokshagundam, D.; Baik, M. H.; Lippard, S. J. *J. Am. Chem. Soc.* **2006**, *128*, 14364–14373.
(44) McQuade, L. E.; Ma, J.; Lowe, G.; Ghatpande, A.; Gelperin, A.; Lippard, S. J. *Proc. Natl. Acad. Sci. U. S. A.* **2010**, *107*, 8525–8530.
(45) Pluth, M. D.; McQuade, L. E.; Lippard, S. J. *Org. Lett.* **2010**, *12*, 2318–2321.
(46) McQuade, L. E.; Pluth, M. D.; Lippard, S. J. *Inorg. Chem.* **2010**, *49*, 8025–8033.
(47) Zhou, Y.; Marcus, E. M.; Haugland, R. P.; Opas, M. *J. Cell. Physiol.* **1995**, *164*, 9–16.
(48) Kuwana, E.; Sevick-Muraca, E. M. *Anal. Chem.* **2003**, *75*, 4325–4329.
(49) Aslan, K.; Lakowicz, J. R.; Szmacinski, H.; Geddes, C. D. *J. Fluoresc.* **2005**, *15*, 37–40.

(50) Nolan, E. M.; Lippard, S. J. *J. Mater. Chem.* **2005**, *15*, 2778–2783.
(51) Nolan, E. M.; Lippard, S. J. *J. Am. Chem. Soc.* **2007**, *129*, 5910–5918.
(52) Salerno, M.; Ajimo, J. J.; Dudley, J. A.; Binzel, K.; Urayama, P. *Anal. Biochem.* **2007**, *362*, 258–267.
(53) Chang, C. J.; Jaworski, J.; Nolan, E. M.; Sheng, M.; Lippard, S. J. *Proc. Natl. Acad. Sci. U. S. A.* **2004**, *101*, 1129–1134.
(54) Nolan, E. M.; Jaworski, J.; Okamoto, K. I.; Hayashi, Y.; Sheng, M.; Lippard, S. J. *J. Am. Chem. Soc.* **2005**, *127*, 16812–16823.
(55) Aravindakumar, C. T.; Ceulemans, J.; De Ley, M. *Biochem. J.* **1999**, *344*, 253–258.
(56) Berendji, D.; KolbBachofen, V.; Meyer, K. L.; Grapenthin, O.; Weber, H.; Wahn, V.; Kroncke, K. D. *FEBS Lett.* **1997**, *405*, 37–41.
(57) Kroncke, K. D.; Fehsel, K.; Schmidt, T.; Zenke, F. T.; Dasting, I.; Wesener, J. R.; Bettermann, H.; Breunig, K. D.; Kolbbachofen, V. *Biochem. Biophys. Res. Commun.* **1994**, *200*, 1105–1110.
(58) Bogdan, C. *Nat. Immunol.* **2001**, *2*, 907–916.
(59) Xue, G. P.; Bradshaw, J. S.; Dalley, N. K.; Savage, P. B.; Krakowiak, K. E.; Izatt, R. M.; Prodi, L.; Montalti, M.; Zaccheroni, N. *Tetrahedron* **2001**, *57*, 7623–7628.
(60) Fahrni, C. J.; O'Halloran, T. V. *J. Am. Chem. Soc.* **1999**, *121*, 11448–11458.
(61) Lim, M. D.; Lorkovic, I. M.; Ford, P. C. In *Methods Enzymology: Nitric Oxide, Part E*: Academic Press: New York, 2005; Vol. 396, pp 3−17.
(62) Rasband, W. S. *ImageJ*; U. S. National Institutes of Health: Bethesda, MD, 1997−2011.
(63) *APEX2, 2008−4.0*; Bruker AXS, Inc.: Madison, WI, 2008.
(64) Sheldrick, G. M. *SADABS: Area-Detector Absorption Correction*; University of Gottingen: Gottingen: Germany, 2008.
(65) Sheldrick, G. M. *SHELXTL-97, 6.14*; University of Gottingen: Gottingen, Germany, 2000.
(66) Sheldrick, G. M. *Acta Crystallogr., Sect. A* **2008**, *64*, 112–122.